Carbohydrate Polymers 117 (2015) 592–599

Contents lists available at ScienceDirect

Carbohydrate Polymers

journal homepage: www.elsevier.com/locate/carbpol

Manipulation the behavior of supramolecular hydrogels of α-cyclodextrin/star-like block copolymer/carbon-based nanomaterials

Jinglin Shen[a], Xia Xin[a,b,*], Yongjie Zhang[c], Lifei Song[a], Lin Wang[a], Weiyue Tang[c], Yingjie Ren[c]

[a] Key Laboratory of Colloid and Interface Chemistry (Shandong University), Ministry of Education, Shanda nanlu No. 27, Jinan 250100, PR China
[b] National Engineering Technology Research Center for Colloidal Materials, Shandong University, Shanda nanlu No. 27, Jinan 250100, PR China
[c] China Research Institute of Daily Chemical Industry, Taiyuan 030001, Shanxi, PR China

ARTICLE INFO

Article history:
Received 8 August 2014
Received in revised form
10 September 2014
Accepted 8 October 2014
Available online 16 October 2014

Keywords:
α-Cyclodextrin
Star-like block copolymer
Graphene
Graphene oxide
Hydrogel

ABSTRACT

A new supramolecular hydrogel self-assembled between α-cyclodextrin (α-CD) and a star-like block copolymer AE73 was prepared. The cooperation effect of complexation of poly-(ethylene oxide) (PEO) segments with α-CD and the hydrophobic interaction between poly-(propylene oxide) (PPO) blocks resulted in the formation of the supramolecular hydrogel with a strong macromolecular network. Then two kinds of carbon materials (graphene and graphene oxide) were successfully incorporated into the above α-CD/AE73 hydrogel to further enhance the mechanical properties. The native hydrogel, as well as hybrid hydrogels, have been thoroughly characterized by using various microscopic techniques, including transmission electron microscopy (TEM), field emission scanning electron microscopy (FE-SEM), Fourier transform infrared (FT-IR) spectroscopy, X-ray diffraction (XRD), thermogravimetric analysis (TGA). Our main purpose is to ascertain whether the properties of the obtained gels depend on these architectures. Interestingly, the phase behavior, the morphology and the mechanical strength of the native hydrogel can be successfully modulated by incorporating graphene and graphene oxide. Taking into account that both PEO/PPO copolymers and α-CD seem to be biocompatible, these gels can be promising for biomedical applications.

© 2014 Elsevier Ltd. All rights reserved.

1. Introduction

Over the past decades, the supramolecular self-assembled aggregates are an important area of soft-materials research and they have attracted much attention because of their high water content and feasible pharmaceutical and biological applications for gene carriers or drug delivery systems (Koopmans & Ritter, 2008; Li et al., 2013; Nebot et al., 2012; Raeburn, Cardoso, Adams, 2013; Roy et al., 2012; Roy, Baral, & Banerjee, 2013; Samanta & Bhattacharya, 2013; van de Manakker, Vermonden, van Nostrum, & Hennink, 2008; Wintgens, Daoud-Mahammed, Gref, Bouteiller, & Amiel, 2008). They are mainly formed from low molecular weight gelators, which manipulate noncovalent interactions such as hydrogen bonding, van der Waals, π–π, and electrostatic interactions to self-assemble and immobilize the solvent into a three-dimensional entangled network in different ways (Long & Hao, 2010; Ran et al., 2011; Zhang & Shen, 2013). Among them, supramolecular cyclodextrins (CDs) gels occupy an important position in self-assemblies, due to the next occurrence of host-guest interaction by the CD cavity in gels for achieving various functions. CDs are natural molecules derived from starch with a relatively hydrophobic cavity (Larrañeta & Isasi, 2014) and they are a series of cyclic oligosaccha-rides composed of 6, 7, and 8 D(+)-glucose units linked by α-1,4-linkages and named α-, β-, and γ-CD, respectively. They have been extensively studied in supramolecular chemistry as host molecules capable of including guest molecules ranging from small organic/inorganic compounds to polymers (Nielsen, Steffensen, & Larsen, 2009; Dodziuk, 2006; Harada, Takashima, & Yamaguchi, 2009; Tan et al., 2012). Among the molecules that produce stable inclusion complexes with cyclodextrins, linear polymers such as PEO and PPO generate polyrotaxane type

* Corresponding author at: Key Laboratory of Colloid and Interface Chemistry, Ministry of Education; National Engineering Technology Research Center for Colloidal Materials, Shandong University, Shanda nanlu No. 27, Jinan, 250100, P. R. China. Phone: +86 531 88363597.
E-mail address: xinx@sdu.edu.cn (X. Xin).

http://dx.doi.org/10.1016/j.carbpol.2014.10.011
0144-8617/© 2014 Elsevier Ltd. All rights reserved.

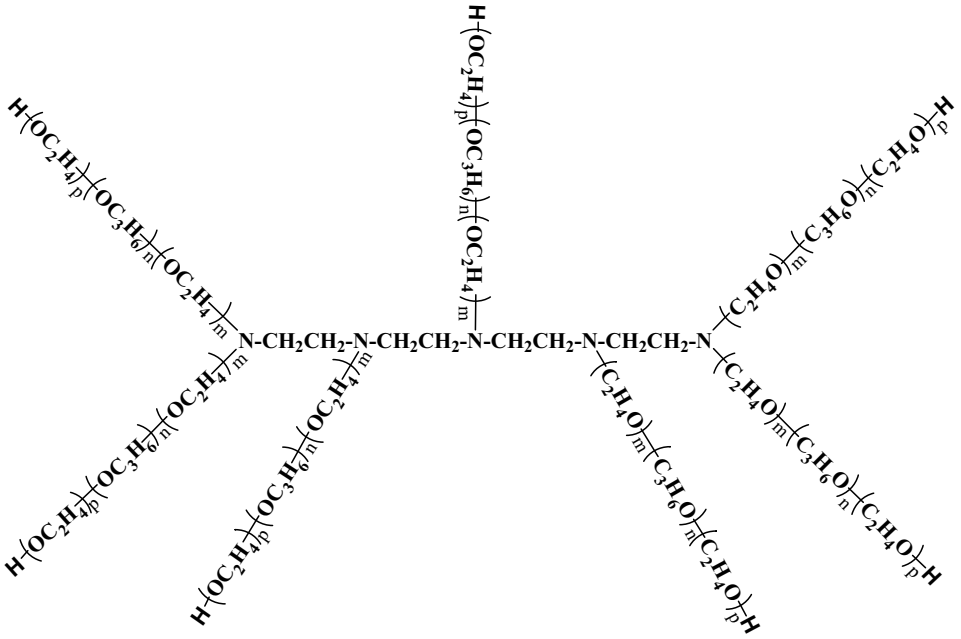

Fig. 1. The chemical structure of star-like block copolymer AE73 (M_w = 10100 g mol^{-1}, PEO% = 49 wt%, m = 8, n = 12, p = 8, cloud point = 37.5 °C).

structures (Harada & Kamachi, 1990). For instance, α-CD molecules yield inclusion complexes with PEO and its block copolymers and cyclodextrins with a wider rim (i.e. β- and γ-CD) are capable of forming complexes with PPO blocks (Li, Li, Zhou, Ni, & Leong, 2001; Ni, Cheng, & Li, 2009; Simões et al., 2013; Huh et al., 2001; Wenz, Han, & Müller, 2006).

Carbon materials have recently attracted significant interest due to its unique mechanical and electrical properties and these newly discovered materials have a wide range of potential applications including transistors, transparent conductors, surfactants, polymer reinforcement, and biodevices (Hu et al., 2010; Kim, Abdala, & Macosko, 2010; Liao, Lin, Macosko, & Haynes, 2011; Liu et al., 2011a; Sun et al., 2008; Yang et al., 2010). Among them, graphene is a two-dimensional structure of sp^2-hybridized carbon atoms arranged in a honey-comb lattice (Geim & Novoselov, 2007), which was first obtained through micromechanical exfoliation of graphite (Gt) in 2004 (Novoselov et al., 2004). Graphene oxide (GO) is a graphene sheet with carboxylic groups at its edges and phenol hydroxyl and epoxide groups on its basal plane (Park & Ruoff, 2009; Compton & Nguyen, 2010). Particularly, GO behaves like an amphiphilic macromolecule with hydrophilic edges and a more hydrophobic basal plane (Guo, Song, & Chen, 2010; Kim et al., 2010b; Zhang, Ren, Wang, & Liu, 2010), which makes it an attractive building block for the construction of various supramolecular architectures (Bai, Li, & Shi, 2011; Xu & Shi, 2011). Previous study has been desmostrated the successfully incorporation of graphene and GO into CD/Pluronic block-copolymers using supra-molecular host–guest complex formation to form graphene based hydrogels (Liu, Chen, & Jiang, 2011; Zu & Han, 2009), where Pluronic block-copolymers served as a surface stabilizer to disperse graphene sheets in aqueous solution and were further utilized to form physical networks through complexation between Pluronic and CD.

In the present work, we synthetized a star-like block copolymer AE73 in our laboratory as the guest molecules and studied the supramolecular assembly in the aqueous solutions of α-CD/AE73. It was discovered that supramolecular hydrogels can be prepared by the assembly of simple α-CD/AE73 inclusion complexes. Then graphene and GO were demonstrated successfully incorporating into the α-CD/AE73 hydrogels. The native hydrogel, as well as hybrid hydrogels, were characterized by transmission electron microscopy (TEM), scanning electron microscopy (FE-SEM), Fourier transform infrared (FT-IR) spectroscopy, X-ray diffraction (XRD), Thermogravimetric analysis (TGA).

2. Experimental

2.1. Materials

α-CD was purchased from Shandong Binzhou Zhiyuan Bio-Technology Co., Ltd. The branched PEO–PPO–PEO block polyether (AE73) was synthesized in our laboratory. Graphene and graphene oxide were obtained from Nanjing XFNANO Materials Tech Co., Ltd. All the above reagents were used without further purification. Water used in the experiments was triply distilled by a quartz water purification system.

2.2. Synthesis and characterization of AE73

AE73 was synthesized by anionic polymerization, as depicted in our previous work (Gong et al., 2011). Tetraethylenepentamine (TEPA) was used as the initiator and potassium hydroxide used as the catalyst. The crude product was dissolved in distilled water and a right amount of acetic acid was added to neutralize the potassium hydroxide. Then the mixed crude product was extracted with dichloromethane and dried in a vacuum oven at 60 °C for 24 h. The molecular structure of AE73 is illustrated in Fig. 1. The average molecular weight of AE73 is 10,100 g mol^{-1} measured by gel permeation chromatography (a GPC system equipped with a Waters binary HPLC pump1525 and a Waters 2414 refractive index detector using HR2, HR3 and HR4 styrogel columns eluted with tetrahydrofuran (1 mL min^{-1}) and the polydispersity is 1.14).

2.3. Preparation of complexes

For graphene dispersions, stock solution of 0.05 wt% AE73 was prepared by dissolving the desired amount of AE73 in water at room temperature. Dispersions of graphene in 0.05 wt% AE73 aqueous solution were obtained by sonicating the mixtures for 2 h at 40 kHz and 250 W using KQ-250DB ultrasonic apparatus (Shanghai). Then, a homogeneous black dispersion was obtained. The as-prepared

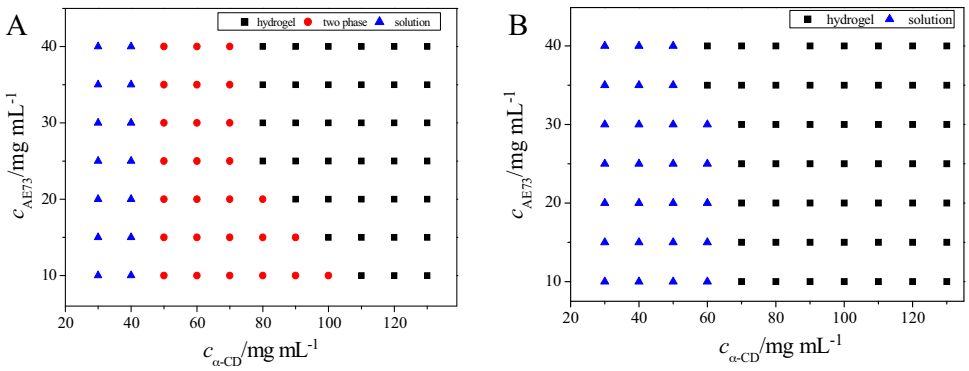

Fig. 2. Phase behavior of (A) α-CD/AE73 and (B) α-CD/AE73/3 mg mL^{-1} GO mixed system after equilibrated at 20.0 ± 0.1 °C for at least 4 weeks.

graphene dispersions contain well-dispersed graphene as well as large aggregates. Small amount of black precipitates were noticed after deposition at room temperature for 2 weeks. The upper phase, which can be stable at room temperature for months, was collected for further use. Graphene oxide can be dispersed in water directly by ultrasonication for 4 h.

All complexes were formed by mixing a determinate amount of AE73 and graphene (or GO) with an aqueous solution of CD by vigorous stirring. Prior to any measurements, the resulting mixtures were kept at room temperature for at least one week.

2.4. Characterizations

TEM observations were carried out on a JEOL JEM-100 CXII (Japan) at an accelerating voltage of 80 kV. FE-SEM observations were carried out on a JSM-6700F.

FTIR spectrum was recorded on a VERTEX-70/70 v spectrometer (Bruker Optics, Germany). XRD patterns of the freeze-dried samples were measured between 1 and 90° in the 2θ scan mode (2.5° min^{-1}) using a Rigaku D/Max 2200-PC diffractometer with Cu *K*a radiation (λ = 0.15418 nm) and a graphite monochromator at room temperature. TGA data were collected using a Universal V3.6 TA Thermal Analysis Q5000 system. The sample was placed in a platinum crucible and heated under a flow of N_2 from ~50 °C to 800 °C at a heating rate of 10 °C min^{-1}.

3. Results and discussion

3.1. Phase behavior of α-CD/AE73 mixed system

First, phase behavior study on α-CD/AE73 mixed system was performed to determine the conditions for gel formation. Despite the formation of micelles, 100 mg mL^{-1} of aqueous solution of both α-CD and AE73 can not form hydrogels. However, aqueous solutions containing 100 mg mL^{-1} α-CD and 15 mg mL^{-1} AE73 formed gels at room temperature. Fig. 2A shows the phase diagram obtained after samples equilibrated at 20.0 ± 0.1 °C for at least two weeks when formation of gels was able to be clearly distinguished and the gelation ability was investigated by an inverted test tube method. Fig. 3(A–E) shows the photos for five typical hydrogels of α-CD/AE73 with 10 mg mL^{-1} AE73 and increasing amount of α-CD. It can be seen from Figs. 2c and 3 that the samples changed that the solution state into two phase state and finally changed into gel state.

It is known that α-CD forms crystalline inclusion complexes with necklace-like supramolecular structure with low molecular weight PEO from aqueous solution (Harada, Li, & Kamachi, 1992). Here the inclusion complexes formed by α-CD and PEO blocks of AE73 are thought to aggregate into microcrystals, which act as physical crosslinks and induce formation of a supramolecular polymer network, consequently resulting in the gelation of the solutions. The micellization of the PPO block is also important in the gelation process. The hydrophobic interactions between the PPO blocks facilitate the formation of the polymer network. Therefore, the gelation of the aqueous solotions of α-CD and AE73 is the result of a cooperation of the inclusion complexation between α-CD and PEO blocks and the micellization of the PPO block of AE73 (Li et al., 2006).

3.2. Dispersion effect of AE73 upon graphene

Because graphene is hydrophobic, so we first should use 0.05 wt% AE73 to disperse it. The dispersion effect of graphene in 0.05 wt% AE73 solution is presented in the inset of Fig. 4A. The samples can be stably stored at room temperature for several months without obvious settlement. It has been well established that PEO–PPO–PEO triblock copolymers impede graphene aggregation mainly by the well-known steric repulsion. When mixed with graphene, the PO groups would interact with the plane of graphene by hydrophobic force while the EO groups would extend into water and hence create a so-called steric repulsion.

Graphene oxide can be dispersed in water directly by ultrasonication. The dispersion effect of graphene oxide in water is presented in the inset of Fig. 4B. Aqueous suspensions of graphene oxide in water are also stable for several months with no precipitation occurring. GO can be dispersed very well in water at the level of individual sheets because of the many oxygen-containing functional groups (such as —COOH and —OH) on the surfaces of GO and electrostatic repulsion between the negative charge of GO sheets (ionization of carboxylic acid and phenolic hydroxyl groups on the

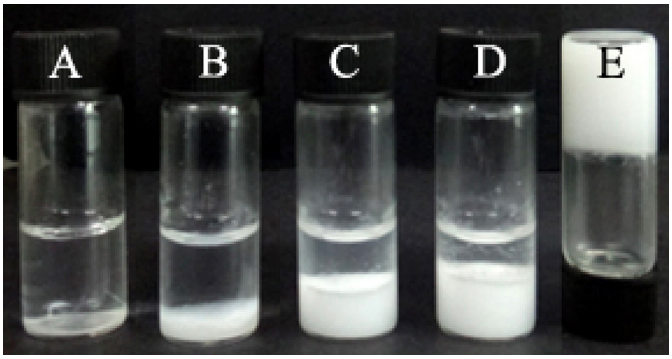

Fig. 3. Photographs of five typical samples: 10 mg mL^{-1} AE73 with varied α-CD concentrations: (A) 30, (B) 50, (C) 70, (D) 90, (E) 110 mg mL^{-1}, respectively. The samples were stored at room temperature for at least two weeks before the photos were taken.

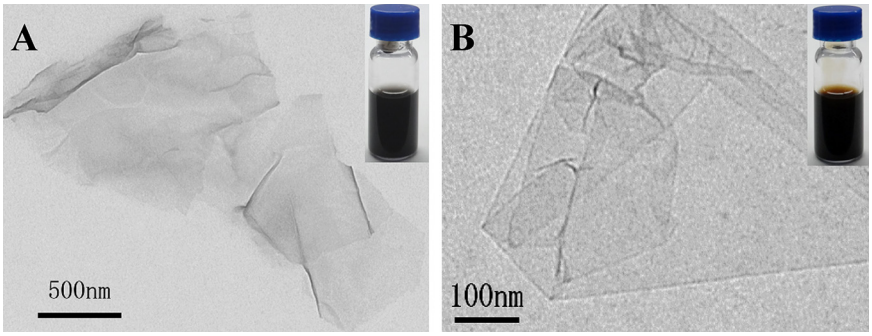

Fig. 4. TEM images of (A) 0.05 wt% AE73-stabilized 0.5 mg mL^{-1} graphene and the inset of A is the photograph of this sample; (B) water-dispersed 5 mg mL^{-1} graphene oxide and the inset of B is the photograph of this sample. The samples were stored at room temperature for at least two weeks before the photos were taken.

GO sheets) (Li, Müller, Gilje, Kaner, & Wallace, 2008). TEM images show that graphene (Fig. 4A) and graphene oxide (Fig. 4B) were fully exfoliated into individual sheets by ultrasonic treatment.

3.3. The effects of graphene and GO on the phase behavior of α-CD/AE73 mixed system

Then, the effects of graphene and GO on the phase behavior of α-CD/AE73 mixed system were investigated. The addition of the graphene can not change the phase behavior of α-CD/AE73 mixed system so much, but the addition of GO greatly changed the properties of the system which is shown in Fig. 2B. The two phase states of α-CD/AE73 mixed system completely disappeared and changed to homogeneous solution and gel phase. For example, one of the two phase state of the sample of 100 mg mL^{-1} α-CD/10 mg mL^{-1} AE73 was selected as shown in Fig. 5A(a). It can be seen that with the incorporation of graphene into this sample, the sample remains two phase state and the graphene was located in the bottom phase (Fig. 5A(b)). But for GO, the GO sheets probably interact well with AE73 without aggregation and at last make the sample become a homogeneous hydrogel (Fig. 5A(c)). It is speculated that the GO sheets act as physical cross-link junctions, toughening the parent hydrogel. That is, the formation of the stable aqueous copolymer-coated GO solutionis due to the non-covalent interaction between the hydrophilic PEO segments of the copolymer and the hydrophilic GO surface. Utilizingthe dual roles of copolymer interaction with GO in aqueous solution and forming supramolecular hydrogel with α-cyclodextrin through the penetration of PEO chains into the cyclodextrin cavities, it can absolutely change the phase behavior of α-CD/AE73 systems and make the interaction strong.

Moreover, GO nanosheets are hydrophilic and contain numerous —COOH and —OH groups, which can form hydrogen bonds with water and thus cause the hydrogel to combine with more water molecules (Zhang et al., 2011). If the hydrogel state of the sample of 100 mg mL^{-1} α-CD/20 mg mL^{-1} AE73 was selected as shown in Fig. 5B (a), it can be seen that with the incorporation of graphene and GO into this sample, the sample remains hydrogel state (Fig. 5B(b) and (c)). The difference between a graphene hydrogel and graphene precipitation is the stacking states of their graphene sheets. Graphene sheets are randomly orientated in a hydrogel, whereas they adopt a parallel arrangement in their precipitation.

3.4. Microstructures of the self-assembled structures

It is generally accepted that the macroscopic properties of the gels are determined by the organization of the subunits in molecular levels. To probe the micro-structures of the gels, TEM

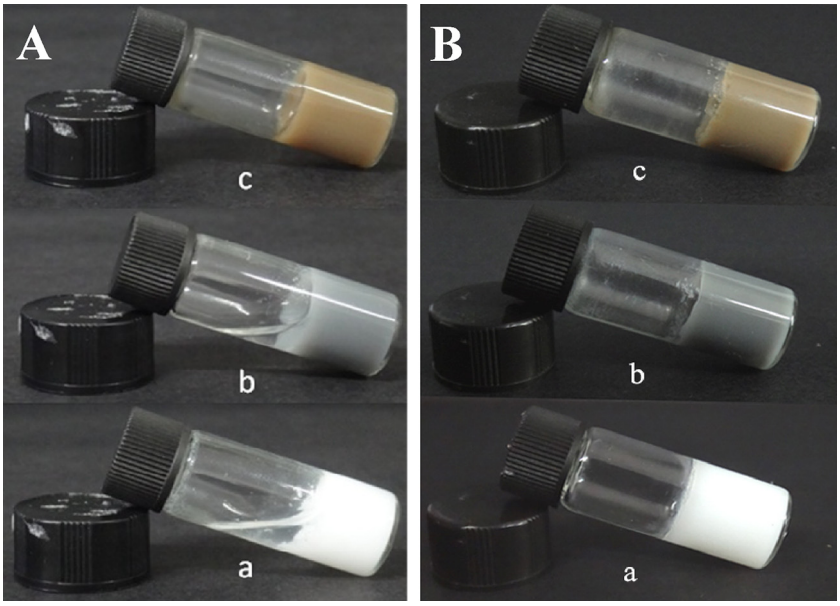

Fig. 5. Photographs of the samples of (A): (a) 100 mg mL^{-1} α-CD/10 mg mL^{-1} AE73, (b) 100 mg mL^{-1} α-CD/10 mg mL^{-1} AE73/0.2 mg mL^{-1} graphene, (c) 100 mg mL^{-1} α-CD/10 mg mL^{-1} AE73/3 mg mL^{-1} GO; (B): (a) 100 mg mL^{-1} α-CD/20 mg mL^{-1} AE73, (b) 100 mg mL^{-1} α-CD/20 mg mL^{-1} AE73/0.2 mg mL^{-1} graphene, (c) 100 mg mL^{-1} α-CD/20 mg mL^{-1} AE73/3 mg mL^{-1} GO. The samples were stored at room temperature for at least two weeks before the photos were taken.

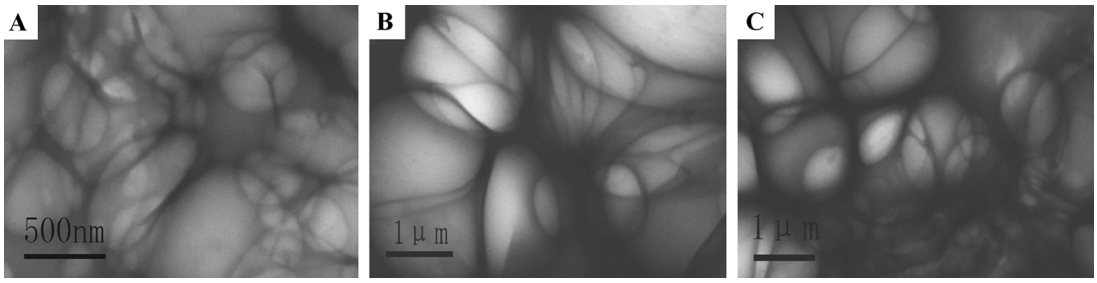

Fig. 6. TEM image of (a) hydrogel of 100 mg mL^{-1} α-CD/20 mg mL^{-1} AE73, (b) hydrogel of 100 mg mL^{-1} α-CD/20 mg mL^{-1} AE73/0.2 mg mL^{-1} graphene, (c) hydrogel of 100 mg mL^{-1} α-CD/20 mg mL^{-1} AE73/3 mg mL^{-1} GO.

observations were carried out (Sun et al., 2014). Fig. 6A shows the morphology of the native 100 mg mL^{-1} α-CD/20 mg mL^{-1} AE73 hydrogel, which indicates the formation of a network of nanofibers. As can be seen in Fig. 6B and C, after the incorporation of graphene and GO into α-CD/AE73 hydrogels, the hydrogels still remain the network structures. But also because of the incorporation of graphene and GO into α-CD/AE73 hydrogels, the morphology of these two kinds of samples are thicker than that of α-CD/AE73 hydrogels under TEM observations.

Then, SEM images were used to furthere characterize the structures of α-CD/AE73/graphene and α-CD/AE73/GO ternary composite hydrogels. First, the lyophilized GO dispersion shows a 3D network composed of a sponge-like GO architecture with pore diameters at the micrometric level and the holes of the samples are uniformly distributed over a large scale sheets as shown in Fig. 7A and B. It is reasonable to conclude that a loose dynamic GO network existed in the original dispersion of GO sheets owing to a force balance between electrostatic repulsion and binding interactions (hydrogen bonding, π-stacking, hydrophobic effect, etc.) (Bai, Li, Wang, & Shi, 2011b). For the freeze dried 0.05 wt% AE73 dispersed 0.5 mg mL^{-1} graphene solution, it can be seen from Fig. 7C and D that because of the lower concentration of graphene and its weak interaction between graphene, the network structure of graphene is not ordered and dense compared with GO.

For the α-CD/AE73 hydrogels, the morphology of the sample shows compact network structure (Fig. 8A and B). After introduction of graphene and GO, the morphologies of the hydrogels were changed. There are filamentous structures with interconnecting pores inside and outside the holes of the hydrogel. Moreover, it is worth noting that the structures of the α-CD/AE73/graphene (Fig. 8C and D) and α-CD/AE73/GO (Fig. 8E and F) hydrogels become denser than that of pure graphene and GO but looser than that of α-CD/AE73 hydrogels. It is attributed to the layered graphene and GO participated in the formation of the network structures and these results further confirmed that the hybrid hydrogel composites were successfully prepared.

3.5. XRD analysis

In order to get information about the degree of crystallinity of α-CD/AE73 xerogels after the graphene and GO nanosheets were incorporated, XRD of the samples was performed and the results are shown in Fig. 9. It can be seen that in Fig. 9A(a), the pattern of α-CD represents a cage type structure. The inclusion complex formation between PEO blocks of the AE73 copolymers and α-CD in the hydrogels (Fig. 9A(b)) shows a number of sharp reflections and the main one at $2\theta = 19.8$ represents the channel type structure of crystalline necklace-like complex of α-CD and PEO, which is totally

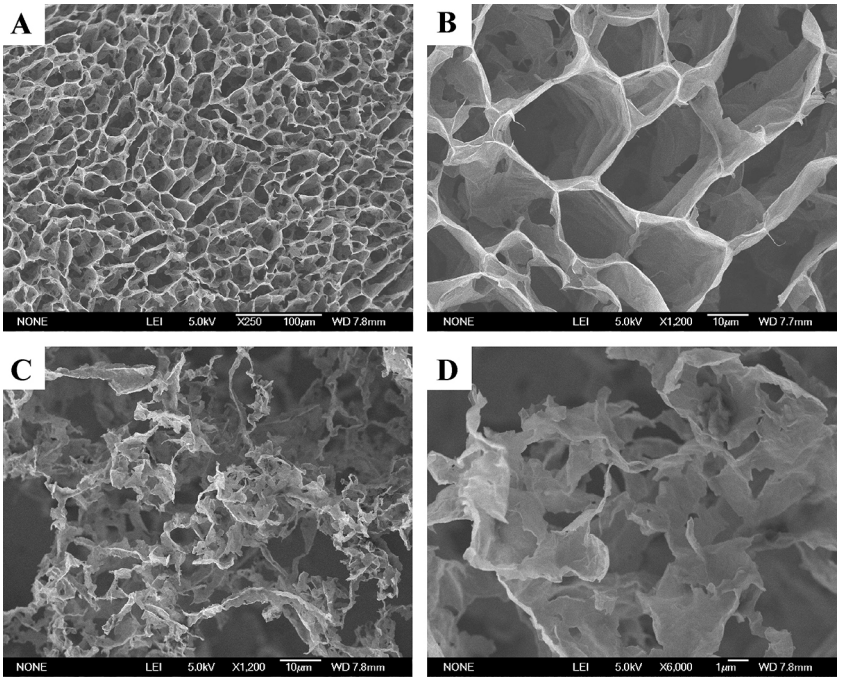

Fig. 7. SEM images of (A) freeze dried GO solution, (B) a local partial enlarged image of (A), (C) freeze-dried 0.05 wt%AE73 dispersed 0.5 mg mL^{-1} graphene solution, (D) a local partial enlarged image of (C).

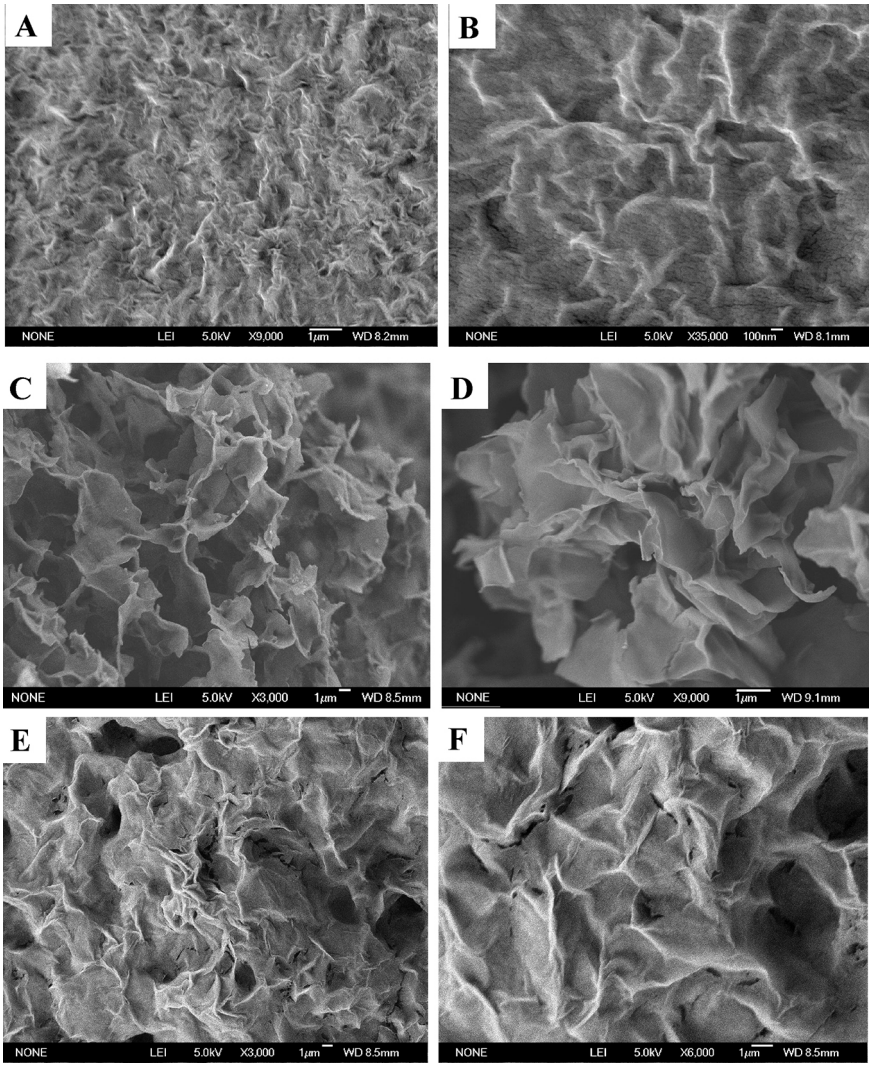

Fig. 8. SEM images of the hydrogels: (A) freeze dried 100 mg mL^{-1} α-CD/20 mg mL^{-1} AE73 hydrogel, (B) a local partial enlarged image of (A), (C) freeze dried 100 mg mL^{-1} α-CD/20 mg mL^{-1} AE73/graphene, (D) a local partial enlarged image of (C), (E) freeze dried 100 mg mL^{-1} α-CD/20 mg mL^{-1} AE73/GO, (F) a local partial enlarged image of (E).

different from that of α-CD (Feng & Zhao, 2003). For the freeze-dried xerogels samples, there are no obvious differences between the α-CD/AE73 xerogels and α-CD/AE73/graphene or GO xerogels (Fig. 9A(c) and (d)). All the samples have similar curves which suggest that the graphene and GO nanosheets do not have a noticeable effect on the degree of crystallinity of the α-CD/AE73 xerogels.

3.6. FT-IR results

FT-IR spectroscopy is a powerful method for characterizing the interactions within supramolecular assemblies and it is powerful enough to detect the hydrogen bond within the region of 1800–400 cm^{-1} (Kawasaki & Maeda, 2001; Wang et al., 2014). It can

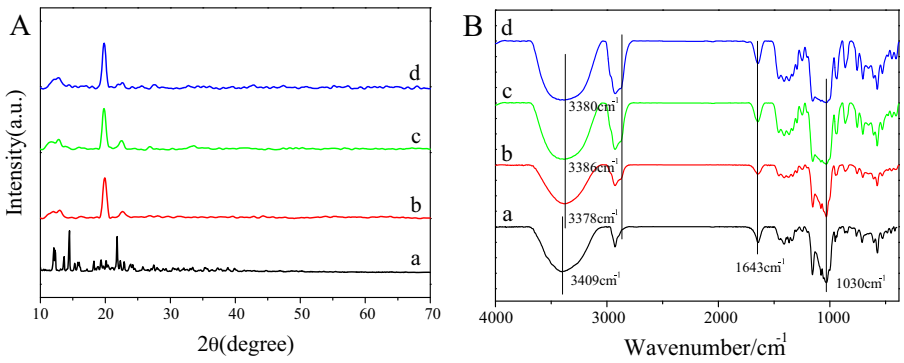

Fig. 9. (A) XRD patterns of (a) α-CD, (b) 100 mg mL^{-1} α-CD/20 mg mL^{-1} AE73, (c) 100 mg mL^{-1} α-CD/20 mg mL^{-1} AE73/0.2 mg mL^{-1} graphene, (d) hydrogel of 100 mg mL^{-1} α-CD/20 mg mL^{-1} AE73/3 mg mL^{-1} GO; (B) FT-IR spectra of the samples: (a) α-CD, (b) 100 mg mL^{-1} α-CD/20 mg mL^{-1} AE73, (c) 100 mg mL^{-1} α-CD/20 mg mL^{-1} AE73/0.2 mg mL^{-1} graphene, (d) hydrogel of 100 mg mL^{-1} α-CD/20 mg mL^{-1} AE73/3 mg mL^{-1} GO.

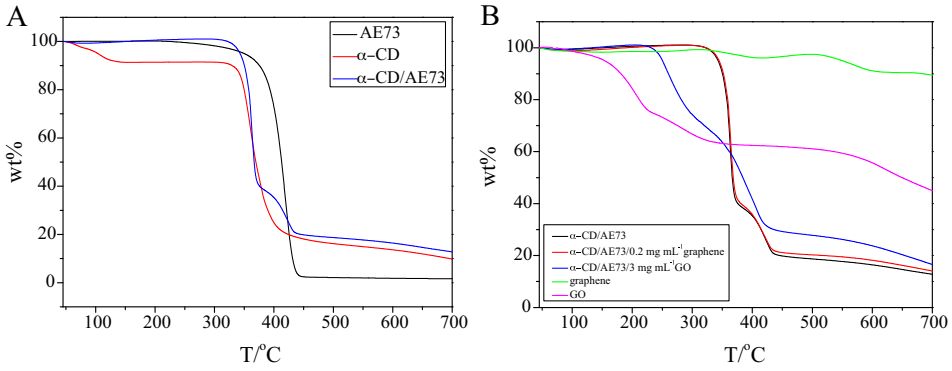

Fig. 10. TGA curve for (A) α-CD, AE73, α-CD/AE73 and (B) α-CD/AE73, graphene, GO, α-CD/AE73/graphenen and α-CD/AE73/GO xerogels which show corresponding degradation temperatures.

be seen from Fig. 9B that the IR spectrum of all the xerogels are very similar to that of α-CD, indicating that the skeleton of the xerogels are mainly consists of α-CD and the hydrogen bonding interactions between adjacent α-CD molecules and between α-CD and water molecules have promoted the formation of supramolecular hydrogels. For all the samples, the wide peak at about 3380–3410 cm^{-1} is well-known for symmetric and antisymmetric O—H stretching modes. Moreover, one could observe that the peak of O—H shifts from 3408 cm^{-1} to a lower frequency at 3386 cm^{-1} for α-CD/AE73/graphene xerogels and 3380 cm^{-1} for α-CD/AE73/GO xerogels (Fig. 9B(a–d)). It can be ascribed that the destruction of hydrogen bonding between α-CD molecules and the formation of new hydrogen bonding between α-CD and graphene (or GO) (or between AE73 and graphene (or GO)) influence the strong and ordered intermolecular interactions. It can be also seen that the asymmetric and symmetric methylene stretching bands are located at 2933 and 2863 cm^{-1}, respectively, and the stretching bands of the methylene units become more apparent when graphene and GO were added. The stretching vibration at 1643 cm^{-1} is related to carbonyl groups and the peak at 1030 cm^{-1} is in agreement with the stretching vibration of C—O bond of α-CD. Moreover, the weak peaks at 1380 cm^{-1} and 1419 cm^{-1} are correlated with the bending vibration of C—H and O—H, respectively.

3.7. TGA analysis

Fig. 10 depicts the TGA of the freeze-dried xerogels. According to the TGA results in Fig. 10A, it can be seen that around 100 °C, the weight loss of α-CD was assigned to the removal of residual water in the sample. The α-CD/AE73 xerogel exhibit a higher thermal stability compared to the pure α-CD and AE73 and it contains two steps of decomposition which are at 318 °C (belong to α-CD) and 370 °C (belong to AE73), respectively. These results suggest the supramolecular interactions originated from the macromer chain of AE 73 threading into the α-CD channel can increase the α-CD thermal stability. Moreover, after the incorporation of GO to the α-CD/AE73 hydrogels, α-CD/AE73/GO xerogels exhibit a higher thermal stability compared to the baseline α-CD/AE73 xerogels because of the restricted mobility of the polymer chains in the presence of GO while α-CD/AE73/graphene xerogels have not so much change compared to the baseline α-CD/AE73 xerogels as shown in Fig. 10B (Das et al., 2013; Jiang, Shen, Wu, & Shen, 2010; Yang, Shang, & Li, 2011).

Furthermore, the viscoelastic properties of these hydrogels were investigated by rheological measurement which are shown in Fig. S1. Our conclusion is that the presence of GO enhances the formation of the gels, while the addition of graphene could weaken the formation of the gels. This indictates that graphene (hydrophobic) and graphene oxide (hydrophilic) have different effects on the formation of hydrogels. Moreover, we also did the experiment for the application in adsorption of dye which are shown in Fig. S2. The results also demonstrated that α-CD/AE73/GO gel has a very good absorption ability of methylene blue, the second is α-CD/AE73/graphene gel, α-CD/AE73 gel almost has no absorption ability. More detailed work is in progress.

4. Conclusions

In conclusion, a series of α-CD/AE73/graphene and α-CD/AE73/GO ternary composites were successfully prepared in this study. First, the inclusion complexes formed by α-CD and PEO blocks of AE73 are thought to aggregate into microcrystals, which act as physical crosslinks and induce formation of a supramolecular polymer network, consequently resulting in the gelation of the solutions. Then, with the addition of GO, it can make two phase states of α-CD/AE73 composite change to hydrogels because of the strong interfacial interaction between GO nanosheets and PEO parts of AE73. Compared with GO, graphene can not induce the phase transition but just formed α-CD/AE73/graphene composites. The experiments performed on these graphene and GO-loadded hydrogels offer a clear picture of the structure and properties of the nanocomposite hydrogels. The stimulus response (such as pH, temperature and other guest molecules) of these hydrogels is in further study. Moreover, the α-CD/AE73/GO ternary composite hydrogel exhibited good adsorption properties for water-soluble dyes. After introducing GO, the dye adsorption capacities of the hydrogel were significantly improved. It is also expected that the mechanically strong α-CD/AE73/GO ternary nanocomposite hydrogels can widen the applications in drug delivery systems and bioengineering.

Acknowledgements

We gratefully acknowledge financial support from the National Natural Science Foundation of China (21203109) and Independent Innovation Foundation of Shandong University (IIFSDU, 2012GN015).

Appendix A. Supplementary data

Supplementary data associated with this article can be found, in the online version, at http://dx.doi.org/10.1016/j.carbpol.2014.10.011.

References

Bai, H., Li, C., & Shi, G. (2011). Functional composite materials based on chemically converted graphene. *Advanced Materials*, *23*, 1089–1115.

Bai, H., Li, C., Wang, X., & Shi, G. (2011). On the gelation of graphene oxide. *The Journal of Physical Chemistry C*, *115*, 5545–5551.
Compton, O. C., & Nguyen, S. T. (2010). Graphene oxide, highly reduced graphene oxide, and graphene: Versatile building blocks for carbon-based materials. *Small*, *6*, 711–723.
Das, S., Irin, F., Ma, L., Bhattacharia, S. K., Hedden, R. C., & Green, M. J. (2013). Rheology and morphology of pristine graphene/polyacrylamide gels. *ACS Applied Materials & Interfaces*, *5*, 8633–8640.
Dodziuk, H. (Ed.). (2006). *Cyclodextrins and their complexes: Chemistry, analytical methods, applications*. Weinheim: Wiley-VCH.
Feng, Z., & Zhao, S. (2003). Synthesis and characterization of biodegradable hydrogels based on photopolymerizable acrylate-terminated CL-PEG-CL macromers with supramolecular assemblies of α-cyclodextrins. *Polymer*, *44*, 5177–5186.
Geim, A. K., & Novoselov, K. S. (2007). The rise of graphene. *Nature Materials*, *6*, 183–191.
Gong, H. J., Xu, G. Y., Liu, T., Pang, J. Y., Dou, W. L., & Xin, X. (2011). Synthesis of block polyethers with various structures and their application in dispersing single-walled carbon nanotubes. *Colloid and Polymer Science*, *289*, 933–942.
Guo, P., Song, H., & Chen, X. (2010). Hollow graphene oxide spheres self-assembled by W/O emulsion. *Journal of Materials Chemistry*, *20*, 4867–4874.
Harada, A., & Kamachi, M. (1990). Complex formation between poly(ethylene glycol) and α-cyclodextrin. *Macromolecules*, *23*, 2821–2823.
Harada, A., Li, J., & Kamachi, M. (1992). The molecular necklace: A rotaxane containing many threaded α-cyclodextrins. *Nature*, *356*, 325–327.
Harada, A., Takashima, Y., & Yamaguchi, H. (2009). Cyclodextrin-based supramolecular polymers. *Chemical Society Reviews*, *38*, 875–882.
Hu, W., Peng, C., Luo, W., Lv, M., Li, X., Li, D., et al. (2010). Graphene-based antibacterial paper. *ACS Nano*, *4*, 4317–4323.
Huh, K. M., Ooya, T., Lee, W. K., Sasaki, S., Kwon, I. C., Jeong, S. Y., et al. (2001). Supramolecular-structured hydrogels showing a reversible phase transition by inclusion complexation between poly(ethylene glycol) grafted dextran and α-cyclodextrin. *Macromolecules*, *34*, 8657–8662.
Jiang, L., Shen, X. P., Wu, J. L., & Shen, K. C. (2010). Preparation and characterization of graphene/poly(vinyl alcohol) nanocomposites. *Journal of Applied Polymer Science*, *118*, 275–279.
Kawasaki, H., & Maeda, H. (2001). FT-IR study on hydrogen bonds between the headgroups of dodecyldimethylamine oxide hemihydrochloride. *Langmuir*, *17*, 2278–2281.
Kim, H., Abdala, A. A., & Macosko, C. W. (2010). Graphene/polymer nanocomposites. *Macromolecules*, *43*, 6515–6530.
Kim, J., Cote, L. J., Kim, F., Yuan, W., Shull, K. R., & Huang, J. (2010). Graphene oxide sheets at interfaces. *Journal of the American Chemical Society*, *132*, 8180–8186.
Koopmans, C., & Ritter, H. (2008). Formation of physical hydrogels via host–guest interactions of β-cyclodextrin polymers and copolymers bearing adamantyl groups. *Macromolecules*, *41*, 7418–7422.
Larrañeta, E., & Isasi, J. R. (2014). Non-covalent hydrogels of cyclodextrins and poloxamines for the controlled release of proteins. *Carbohydrate Polymers*, *102*, 674–681.
Li, D., Müller, M. B., Gilje, S., Kaner, R. B., & Wallace, G. G. (2008). Processable aqueous dispersions of graphene nanosheets. *Nature Nanotechnology*, *3*, 101–105.
Li, J., Li, X., Zhou, Z., Ni, X., & Leong, K. W. (2001). Formation of supramolecular hydrogels induced by inclusion complexation between pluronics and α-cyclodextrin. *Macromolecules*, *34*, 7236–7237.
Li, J., Li, X., Ni, X., Wang, X., Li, H., & Leong, K. W. (2006). Self-assembled supramolecular hydrogels formed by biodegradable PEO–PHB–PEO triblock copolymers and α-cyclodextrin for controlled drug delivery. *Biomaterials*, *27*, 4132–4140.
Li, Y., Huang, G., Zhang, X., Li, B., Chen, Y., Lu, T., et al. (2013). Magnetic hydrogels and their potential biomedical applications. *Advanced Functional Materials*, *23*, 660–672.
Liao, K. H., Lin, Y. S., Macosko, C. W., & Haynes, C. L. (2011). Cytotoxicity of graphene oxide and graphene in human erythrocytes and skin fibroblasts. *ACS Applied Materials & Interfaces*, *3*, 2607–2615.
Liu, S., Zeng, T. H., Hofmann, M., Burcombe, E., Wei, J., Jiang, R., et al. (2011). Antibacterial activity of graphite, graphite oxide, graphene oxide, and reduced graphene oxide: Membrane and oxidative stress. *ACS Nano*, *5*, 6971–6980.
Liu, J., Chen, G., & Jiang, M. (2011). Supramolecular hybrid hydrogels from noncovalently functionalized graphene with block copolymers. *Macromolecules*, *44*, 7682–7691.
Long, P., & Hao, J. (2010). A gel state from densely packed multilamellar vesicles in the crystalline state. *Soft Matter*, *6*, 4350–4356.
Nebot, V. J., Armengol, J., Smets, J., Prieto, S. F., Escuder, B., & Miravet, J. F. (2012). Molecular hydrogels from bolaform amino acid derivatives: A structure-properties study based on the thermodynamics of gel solubilization. *Chemistry—A European Journal*, *18*, 4063–4072.
Ni, X., Cheng, A., & Li, J. (2009). Supramolecular hydrogels based on self-assembly between PEO–PPO–PEO triblock copolymers and α-cyclodextrin. *Journal of Biomedical Materials Research, A*, *88*, 1031–1036.
Nielsen, A. L., Steffensen, K., & Larsen, K. L. (2009). Self-assembling microparticles with controllable disruption properties based on cyclodextrin interactions. *Colloids and Surfaces B: Biointerfaces*, *73*, 267–275.
Novoselov, K. S., Geim, A. K., Morozov, S. V., Jiang, D., Zhang, Y., Dubonos, S. V., et al. (2004). Electric field effect in atomically thin carbon films. *Science*, *306*, 666–669.
Park, S., & Ruoff, R. S. (2009). Chemical methods for the production of graphenes. *Nature Nanotechnology*, *4*, 217–224.
Raeburn, J., Cardoso, A., & Adams, D. (2013). The importance of the self-assembly process to control mechanical properties of low molecular weight hydrogels. *Chemical Society Reviews*, *42*, 5143–5156.
Ran, X., Wang, H., Zhang, P., Bai, B., Zhao, C., Yu, Z., et al. (2011). Photo-induced fiber–vesicle morphological change in an organogel based on an azophenyl hydrazide derivative. *Soft Matter*, *7*, 8561–8566.
Roy, S., Javid, N., Frederix, P. W., Lamprou, D. A., Urquhart, A. J., Hunt, N. T., et al. (2012). Dramatic specific-ion effect in supramolecular hydrogels. *Chemistry—A European Journal*, *18*, 11723–11731.
Roy, S., Baral, A., & Banerjee, A. (2013). An amino-acid-based self-healing hydrogel: Modulation of the self-healing properties by incorporating carbon-based nanomaterials. *Chemistry—A European Journal*, *19*, 14950–14957.
Samanta, S., & Bhattacharya, S. (2013). Excellent chirality transcription in two-component photochromic organogels assembled through J-aggregation. *Chemical Communications*, *49*, 1425–1427.
Simões, S., Veiga, F., Torres-Labandeira, J. J., Ribeiro, A. C. F., Concheiro, A., & Alvarez-Lorenzo, C. (2013). Poloxamine–cyclodextrin–simvastatin supramolecular systems promote osteoblast differentiation of mesenchymal stem cells. *Macromolecular Bioscience*, *13*, 723–734.
Sun, X., Liu, Z., Welsher, K., Robinson, J. T., Goodwin, A., Zaric, S., et al. (2008). Nano-graphene oxide for cellular imaging and drug delivery. *Nano Research*, *1*, 203–212.
Sun, X., Xin, X., Tang, N., Guo, L., Wang, L., & Xu, G. (2014). Manipulation of the gel behavior of biological surfactant sodium deoxycholate by amino acids. *The Journal of Physical Chemistry B*, *118*, 824–832.
Tan, L., Liu, Y., Ha, W., Ding, L. S., Peng, S. L., Zhang, S., et al. (2012). Stimuli-induced gel–sol transition of multi-sensitive supramolecular β-cyclodextrin grafted alginate/ferrocene modified pluronic hydrogel. *Soft Matter*, *8*, 5746–5749.
van de Manakker, F., Vermonden, T., van Nostrum, C., & Hennink, W. (2008). Self-assembling hydrogels based on beta-cyclodextrin/cholesterol inclusion complexes. *Macromolecules*, *41*, 1766–1773.
Wang, Y., Xin, X., Li, W., Jia, C., Wang, L., Shen, J., et al. (2014). Studies on the gel behavior and luminescence properties of biological surfactant sodium deoxycholate/rare-earth salts mixed systems. *Journal of Colloid and Interface Science*, *431*, 82–89.
Wenz, G., Han, B. H., & Müller, A. (2006). Cyclodextrin rotaxanes and polyrotaxanes. *Chemical Reviews*, *106*, 782–817.
Wintgens, V., Daoud-Mahammed, S., Gref, R., Bouteiller, L., & Amiel, C. (2008). Aqueous polysaccharide associations mediated by β-cyclodextrin polymers. *Biomacromolecules*, *9*, 1434–1442.
Xu, Y., & Shi, G. (2011). Assembly of chemically modified graphene: Methods and applications. *Journal of Materials Chemistry*, *21*, 3311–3323.
Yang, K., Zhang, S., Zhang, G., Sun, X., Lee, S. T., & Liu, Z. (2010). Graphene in mice: Ultrahigh in vivo tumor uptake and efficient photothermal therapy. *Nano Letters*, *10*, 3318–3323.
Yang, X., Shang, S., & Li, L. (2011). Layer-structured poly(vinyl alcohol)/graphene oxide nanocomposites with improved thermal and mechanical properties. *Journal of Applied Polymer Science*, *120*, 1355–1360.
Zhang, C., Ren, L., Wang, X., & Liu, T. (2010). Graphene oxide-assisted dispersion of pristine multiwalled carbon nanotubes in aqueous media. *The Journal of Physical Chemistry C*, *114*, 11435–11440.
Zhang, L., Wang, Z., Xu, C., Li, Y., Gao, J., Wang, W., et al. (2011). High strength graphene oxide/polyvinyl alcohol composite hydrogels. *Journal of Materials Chemistry*, *21*, 10399–10406.
Zhang, J., & Shen, X. (2013). Temperature-induced reversible transition between vesicle and supramolecular hydrogel in the aqueous ionic liquid-β-cyclodextrin system. *The Journal of Physical Chemistry B*, *117*, 1451–1457.
Zu, S. Z., & Han, B. H. (2009). Aqueous dispersion of graphene sheets stabilized by pluronic copolymers: Formation of supramolecular hydrogel. *The Journal of Physical Chemistry C*, *113*, 13651–13657.